# A novel received signal strength indicator method for modeling Massive MIMO beamforming via multi-task deep learning

**Ibrahim El-Metwally Ramadan[1], Eman AbdElHalim[2], Ahmed Ibrahim Saleh[3], Hossam El-Din Salah Moustafa[2]**

[1]Department of Communications and Electronics, Misr Higher Institute for Engineering and Technology, Mansoura, Egypt
[2]Department of Electronics and Communications Engineering, Faculty of Engineering, Mansoura University, Mansoura, Egypt
[3]Department of Computer Engineering and Systems, Faculty of Engineering, Mansoura University, Mansoura, Egypt

## Article Info

## ABSTRACT

To achieve the best performance in terms of accuracy and complexity of massive multiple-input multiple-output (Massive MIMO) in wireless communication systems, hybrid beamforming (HBF) is a promising technique that provides high data rate multiplexing gains and enhances the spectral efficiency (SE) of the system. In this paper, a novel received signal strength indicator (RSSI) method is proposed to design an HBF for Massive MIMO BF via multitasking deep learning (DL) that minimizes the reliance on the channel state information (CSI) feedback. The trade-off between the enhancement SE of the system and the deep neural networks (DNNs) performance is optimized, and the results reveal that the proposed novel DL techniques achieve predicted spectral efficiencies with accuracy of 99.23% and 95.64% for Deep-HBF and Deep-AFP, respectively. The processing times for Deep-HBF and Deep-AFP are 709.2914 sec and 1425.864 sec, respectively. Notably, Deep-AFP exhibits a higher range of computational complexity compared to Deep-HBF. It is worth mentioning that the proposed techniques utilize the same DNN architecture.

## Corresponding Author:

Ibrahim El-Metwally Ramadan
Department of Communications and Electronics, Misr Higher Institute for Engineering and Technology
Mansoura, Egypt
Email: i.elmatwally89@gmail.com

## 1. INTRODUCTION

Nowadays, many researchers are seeking to explore new advanced methodologies and technologies in fifth generation (5G) mobile networks, to support data traffic with less power consumption and better quality of service (QoS). Therefore, some enabling technologies, such as Massive MIMO technologies, heterogeneous networks (HetNets), and millimeter wave (mmWave) technologies have been identified to achieve a 5G mobile network [1]. Wireless access technologies Massive MIMO antenna array systems are the main enabling technologies for current and future wireless communication systems [2]. It is used for increasing data rates, multiplexing gains, and enhancement of the SE of the system, which can enhance the area throughput. These benefits can be achieved by using these technologies in different propagation environments. However, the using of very large numbers of antennas poses critical challenges for a Massive MIMO system in enhancing system reliability, enabling low-complexity base station coordination, and highly mobile users [3], [4]. Beamforming (BF) is one of the most practical solutions to overcome high path loss and atmospheric attenuation in mm-Wave ranges [5]. How to implement it is a matter of great importance to the radio frequency (RF) industry due to the conflicting requirements for efficiency and flexibility. In the trade-off between cost, size, and complexity, analog and digital BF modulation are combined to generate a

hybrid solution, a preferred architecture in current 5G Massive MIMO systems. However, digital BF is inevitably the direction of the future, and it is only a matter of time before they are used in 5G networks at high bands as well [6], [7]. This technology is based on new versions of artificial neural networks (ANNs) which are called DNNs [8]. It is assumed that DNN performance generally outperforms classical ANN performance at the expense of greater training time, which can be reduced by using advanced hardware (e.g., GPU), and/or proprietary techniques (e.g., transfer learning). DNN design is critical to the success of one of these architectures called convolutional neural networks (CNNs) which have a large number of layers, and nodes and need less pre-processing compared to other classification schemes [9].

Recently, interesting and important can be introduced applications in mm-wave and Massive MIMO systems using DL technologies [10]. Which can generally be used in large training associated with large channel arrays and system feedback. However, these channels are intuitively some environmental engineering functions, building materials, and transmission/reception sites. This was motivated by the use of machine/DL tools that take advantage of low generic features of the environment and user settings and learn how to use them for prediction of the channels/beams of Massive MIMO systems, proactive handoff, enhance system reliability and enable low-complexity base station coordination [11], [12]. DL has been revolutionizing many areas of research as it has the potential to learn better models from large amounts of data. It can be able to solve problems in telecommunication systems [13]. The unique DL network architecture can approximate any function under specific conditions, eliminate the complexity caused by many iterations, and perform real-time calculations to solve the BF design [14] optimization problem. Therefore, this technique is a good way to solve complex optimization problems [15]. Although the training process takes a long processing time, the training takes place in an offline mode. Therefore, DL technology is an effective way to reduce cellular network delay. Hence, in [16] a predictive network for BF in the offline mode was proposed. In studies [17] and [18], a supervised learning-based method was proposed for offline DNN training. When working on the design of BF, we had difficulty finding a suitable optimizer that departed from traditional methods. Therefore, we resorted to using additional computing resources called unsupervised learning instead of supervised learning labels in BF design and training problems to improve the BF design to increase the sum rate at which it can be achieved.

In this paper, the provided methodology proposes the utilization of a trained and optimized received signal strength indicator (RSSI) for modeling Massive MIMO BF systems. This is accomplished through a multi-task DL approach, as depicted in Figure 1. The key aspect of this approach is the use of an unsupervised deep neural network (UDNN) to significantly enhance the SE of the system, which is trained and evaluated using only the RSSI as input. To achieve this, the quantized RSSIs are utilized as inputs for the DNN architecture, thereby eliminating the need for channel state information (CSI). CSI is only used for computing the loss function to update the weight of the UDNN. This allows for obtaining a simplified form for Massive MIMO, focusing on achieving the best design of precoders (analog/digital). The classification and regression tasks in the proposed model relate to accurately determining the optimal precoding schemes for the system. By following this methodology, the aim is to maximize the accuracy of the proposed model, ultimately leading to improved design and performance of precoders in Massive MIMO BF systems. Accordingly, the following points explain the results of the study: i) Providing a comprehensive framework for designing Massive MIMO BF; ii) Achieving a novel DL technique based on the RSSI model to minimize CSI feedback; iii) Proposing a novel DL technique that achieves predicted SE with high accuracy for the BF methods; iv) Building a reliable DL model by splitting the dataset into training, validation, and test sets to give better model accuracy; and v) Calculating the processing times of each BF method.
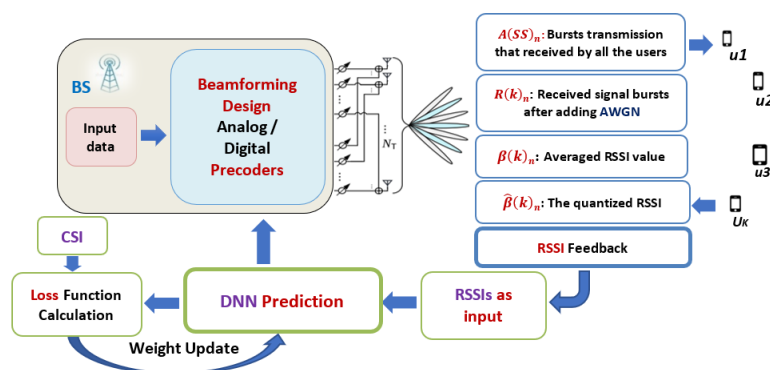


Figure 1. The structure of the proposed system for Massive MIMO BF

## 2.    MATERIAL AND METHOD

This section is structured into three distinct parts. The acquisition process for the DeepMIMO 3D modeling of the Urban Environment mm-Wave/Ma-MIMO channel dataset is described in the first section 2.1. A BF design method based on the RSSI model is described in the second section 2.2. The third section 2.3 presents a suggested framework for Massive MIMO BF modeling. This framework integrates two types of BF approaches using the RSSI model as the foundation for the BF process.

### 2.1.  Channel model and dataset generation

A generic mm-Wave/Massive MIMO channel dataset known as DeepMIMO 3D modeling of the urban environment dataset, is used for generating the training and testing dataset. The generation of the DeepMIMO channels is based on ray tracing data obtained accurately from "Remcom Wireless InSite" [19]. The generation process entails implementing an outdoor tracing scenario labeled "O1". This scenario involves 18 base stations and a total of 1,184,923 users, as depicted in Figure 2. The "O1" scenario is two streets surrounded by buildings with one intersection between them where many random users are placed, with a top view as shown in Figure 2(a). The intersection of two perpendicular streets is placed in the middle of the map. The horizontal is 40 m wide and 600 m long, and the vertical is the same wide and 440 m long as shown in the model [20]. Additionally, the users are distributed in three x-y grids, as illustrated in Figure 2(b). There are 181 users per row in the first grid, which has 2751 rows (designated as R1 through R2751). The second grid, which is represented in Figure 2, has 1101 rows with 181 users each, ranging from R2752 to R3852. From R3853 to R5203, the third grid consists of 1,351 rows, each containing 361 users. Finally, each user is outfitted with a single dipole antenna, and the antenna's axis aligns with the z-direction.
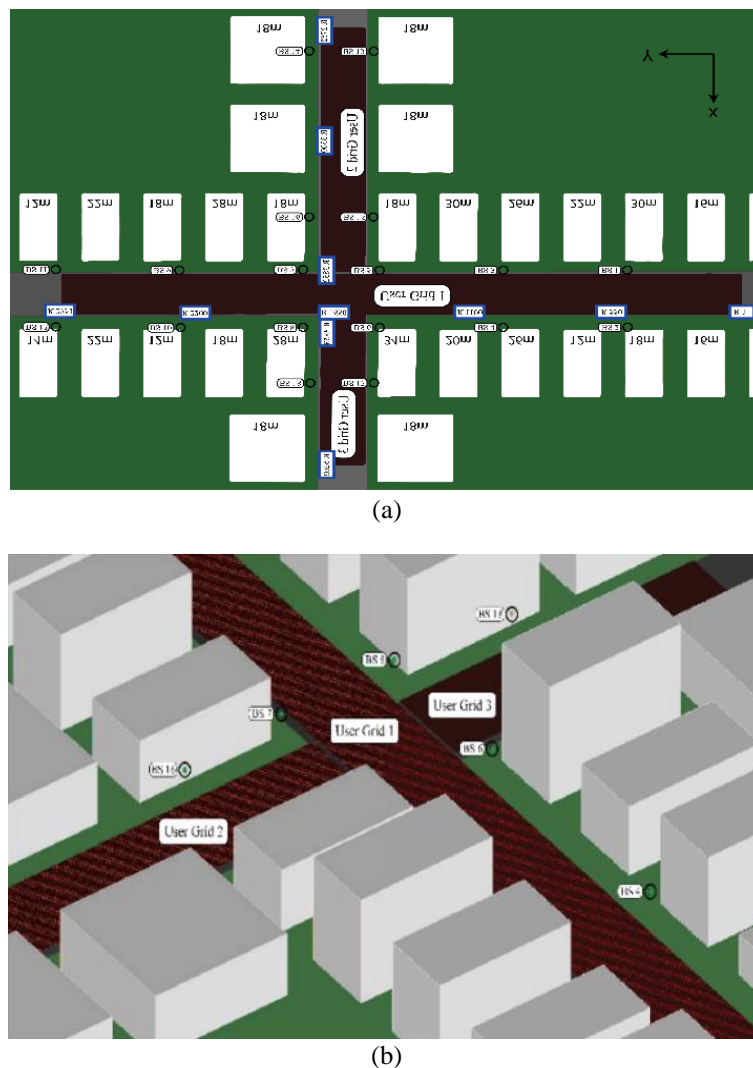


(a)



(b)

Figure 2. 'O1': Model channel scenario (a) top view of the model and (b) bird's-eye view of the model

From this model, the channel vector h with length $N_T$ can be obtained for each user location on a quantized network, and then the channel matrix H ($N_T \times N_k$) into the dataset which can be obtained by concatenating the randomly selected $N_k$ channel vectors of 54,481 potential user locations on the master street of the considered limited area [21]. The channel parameters for this model can be summarized as shown in Table 1. Through synchro signal burst (SSB), which maximizes the information exchanged between users and the BS, the design of a matrix of quantitative RSSIs was obtained, which provides complete information about CSI with a small amount of data that will be sent in the feedback channel. After being able to calculate the RSSI values, the RSSIs are trained by the CNN to have an optimal design for the precoders (analog precoder (AP), digital precoder (DP), and fully digital precoder (FDP)) that maximizes the sum rate of the system.

Table 1. Channel parameters for the DeepMIMO dataset

| Parameter | System | | | | No. of BS Antennas | | | | Users for Area | | |
| | Ray-tracing scenario | Bandwidth (BW) | Num-Subcarriers-OFDM | Num_paths | Num-UPA-ant-x | Num -UPA-ant-y | Num-UPA-ant-z | Ant_spacing | Active-BS | Active-user-first | Active-user-last |
| --- | --- | --- | --- | --- | --- | --- | --- | --- | --- | --- | --- |
| Value | "O1" | 0.5 GHz | 1024 | 10 | 1 | 8 | 8 | 0.5 | 7 | 1000 | 1300 |

## 2.2. Beamforming design based on the RSSI model

The proposed structure of the system for Massive MIMO BF depends on the proposed DNN network that is used to evaluate by using the RSSIs as input to dramatically increase SE, as minimal CSI feedback is required. The training dataset of RSSIs used to design the analog precoder (AP) in the classification task by using the codebook and design the digital precoder (DP) in the regression task. We can get optimum accuracy for the system as related to the design of precoders then the data can be downloaded to each user as illustrated in Figure 1. Three main steps of beam training must be followed to obtain the quantized RSSIs as shown in Figure 1. In the first step, synchronization signal (SS) bursts are transmitted as the base station (BS) sends $n$ SS bursts, where each $n$ burst uses different analog precoders $A(SS)_n$ with a 2-bit phase shift [22]. In the cell, SS $A(SS)_n$ is received for all users. As a result, the received signal $R(k)_n$ for $n^{th}$ bursts after adding the channel model with additive white Gaussian noise $G_N(k)_n$ can be defined as:

$$R(k)_n = H(k)_n A(SS)_n + G_N(k)_n \tag{1}$$

where $H(k)_n$ denotes the channel vector from the $N_T$ antennas at the BS of user $u$. In the second step, which is called RSSI feedback, the average value of RSSI $\beta(k)_n$ is measured for the $n^{th}$ SS burs after receiving $R(k)_n$ by the $k^{th}$ user.

$$\beta(k)_n = \mid H(k)_n A(SS)_n \mid^2 + N^2 \tag{2}$$

where $N^2$ is the power spectral density for AWGN. Through a dedicated error-free feedback channel, all RSSI values from each user are sent to the BS. These first two steps correspond to establishing initial access between BS and all users. RSSIs have to be specified due to the limited accuracy of the measurements and limitations in the feedback channel in practical systems. Therefore, the linear quantization has been used then, we specify $\hat{\beta}(k)_n$ as the user $u$ quantized the RSSI vector sent to the BS [23].

$$\hat{\beta}(k)_n = \frac{Round[\beta(k)_n(2^{N_b}-1)]}{(2^{N_b}-1)} \tag{3}$$

where $N_b$ is the No. of quantization bit. Downlink the data is the final step where the BS downlinks the data to each user location.

### 2.2.1. Hybrid beamforming design (Deep-HBF)

The purpose of BF is to achieve better coverage due to the provision of amplitude/phase variation with the help of an antenna array [24]. The design of the hybrid fully connected BF type combines analog and digital BF techniques. In a single-cell multiple-antenna system, the M single-antenna users are served by providing the BS with $N_T$ antennas and $N_{RF}$ RF chains. The aim of all hybrid BF architectures within Massive MIMO systems is to reduce the complexity of hardware and signals processing, as it provides optimal performance, i.e. near the pure digital performance of purely digital BF. The benefits of this

technology are that it can be used on mm-wave frequencies, providing digital flexibility by being able to dynamically configure many beams and nulls without any hardware change [25]. Just a complete RF chain per array provides extreme flexibility with the number of beams and nulls. Which provides a large number of beams, achieves a high data rate, and improves SE [26]. The user index u of each data symbol can be encoded by designing the matrix of DP ($W$). The AP is designed and applies to all users to send $N_{RF}$ RF series output to $N_T$ antennas. An AP($A$) was obtained from codebook A, which consists of analog beam codewords $l$ for reducing the complexity of the HBF architecture. The SINR of the $k^{th}$ signal received by the user for a given HBF is then expressed as (4) [22].

$$SINR(A, W_k) = \frac{|H(U)_K A_l W_k|^2}{\sum_{j \neq k} |H(U)_K A_l W_j|^2 + N^2} \tag{4}$$

Then the SE of this system is obtained by sum rate evaluation that is expressed as (5) [27].

$$SR(A, W) = \sum_{k=1}^{N_k} log_2 (1 + SNR(A, W_k)) \tag{5}$$

The entire CSI was used for the calculation of the unsupervised loss function. The loss function has been only used for training DP and AP without any objective. RSSIs have only been used at the BS and CSI cannot be accessed by the BS. In this approach, both AP and DP tasks have been designed by training the DNN for the HBF approach. The loss is determined as (6) [23].

$$l_{Deep-HBF} = -\sum_{i=1}^{l} P_l \; SR(A_l, W^*) \tag{6}$$

$P_l$ is an AP output vector, $is$ the $l^{th}$ AP of the codebook, and $W^*$ as DP output.

### 2.2.2. Fully digital precoder design (Deep-AFP)

By taking advantage of massive array gain, to overcome the severe loss path experienced by the propagation channel, analog BF has been proposed as a practical solution to this problem. Analog BF also has lower hardware requirements and thus consumes less power; Therefore, it is favorable compared to the full digital configuration in terms of hardware complexity and power consumption in Massive MIMO [27], [28]. Compared to the SE gain provided by the full digital beam configuration, the link budget has been considered more significant. Designing this type of profile is a complex task as each RF series of each antenna. This approach maintains compatibility between analog and digital precoders. So, we must have a design DP from FDP ($F$) and AP ($A_l$) based on the DNN prediction, the DP ($W_l$) was calculated if we specify:

$$W_l = A_l \; F \tag{7}$$

To compute the loss function of this approach. The FDP and AP must be obtained and then DP can be calculated. If we specify [23]:

$$SR(U) = \sum_{k=1}^{N_k} log_2 \left( 1 + \frac{|H(U)_K F_k|^2}{\sum_{j \neq k} |H(U)_K F_k|^2 + N^2} \right) \tag{8}$$

The FDP loss is expressed as (9) [23]:

$$loss_{FDP} = -SR(U^*) \tag{9}$$

where U$^*$ is the FDP output vector. The AP loss is expressed as (10) [23]:

$$loss_{AP} = -\sum_{i=1}^{l} P_l \; SR(A_l, W_l^*) \tag{10}$$

where $A_l$ is the $l^{th}$ AP of the codebook, and $W_l^*$ is the DP output. The total loss for Deep-AFP is expressed as (11):

$$l_{Deep_{AFP}} = loss_{FDP} + loss_{AP} \tag{11}$$

## 2.3. The DNN framework and architecture for bf design via multi-task DL based on the RSSI method

There are two approaches to dealing with a BF problem. The proposed model is designed to train the BS for an optimal architecture of BF-based RSSI inputs. The DNN model has been used to optimize the weights of the AP and DP. The weights of precoders can be updated based on the loss calculation for each iteration. In the first one, a DNN (Deep-HBF) is designed for prediction AP in a classification task and DP in a regression task. In the other approach, the DNN (Deep-AFP) predicts the analog from the codebook in the classification task directly predicts FDP in the regression task, and then computes the digital precoder using the pseudo inverse. The DNN framework and architecture for two approaches of BF contains the following three main stages as shown in Figure 3. First, the type of BF is chosen and then the quantized RSSIs for the CNN structure are entered. Secondly, the data is trained by the CNN network and Nadam algorithm as network optimizers. Finally, we can evaluate the accuracy of the optimized structure of the system in classification and regression tasks.

After the users can measure the RSSIs, BS will receive the quantized RSSIs, $\hat{\beta}(k)_n = [\hat{\beta}(U_1) \dots \dots \dots \hat{\beta}(U_k)]$ through an allotment free of the errors feedback channel. These input values are then processed by a neural network architecture consisting of a series of three convolutional layers (CL), and two pooling layers. The first CL has 32 layers, the second CL has 64 layers and the third CL has 64 layers, each of them having the LeakyReLU as an activation function [29]. Convolutional layers are interspersed with max pooling layers. Then followed by two fully connected layers (FCL) layers, each of which has 4069 neurons and has the ReLU as an activation function [30]. Then followed by an output layer for each task. The first task is a regression task for FDP and DP and the second task is a classification task for AP in each network.
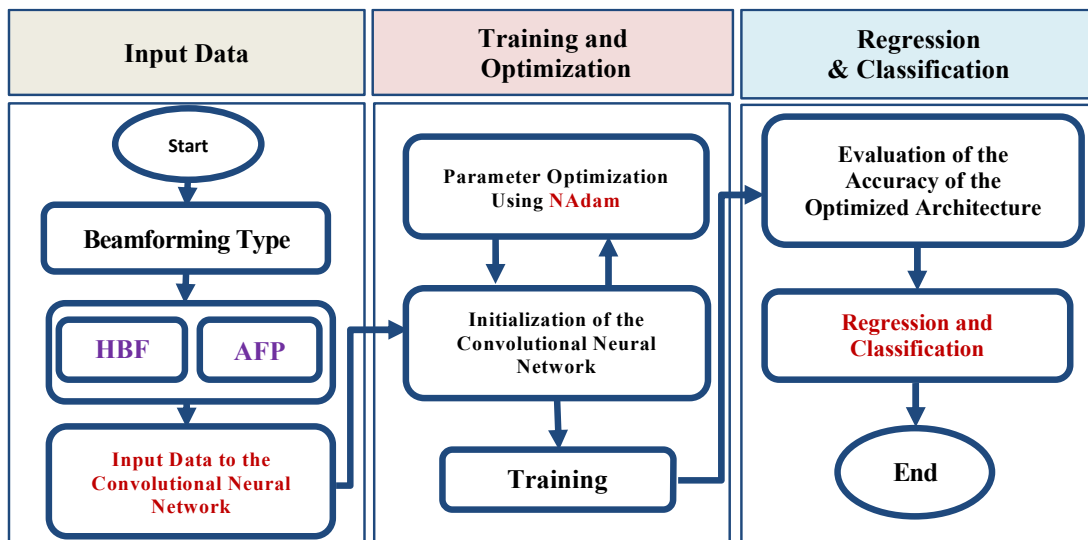


Figure 3. DNN framework and architecture

Both approaches of BF have the same dimensions as the AP task and are equal to the size of the codebook ($l = N_{CB}$). The real and imaginary parts of the output will be separated and the output layer dimension of the DP task in Deep-HBF is ($2 \times N_{CB} \times N_{RF}$), and ($2 \times N_k \times N_T$) for the FDP task in Deep-AFP. Batch normalization can be used to reduce internal variable transformation and speed up learning. To avert the over-regulation problem, the dropout probability of all layers was set to the value of (0:05). The activation function for classifying the layer is SoftMax [30]. The activation function for the regression layer is defined as a linear function [31]. Finally, the "Nadam" algorithm has been used as a network optimizer, having coefficients $\beta_1$, and $\beta_2$ were used for computing running averages of the gradient and its square. The "ReduceLROnPlateau" is used to schedule the reduction of the learning rate. Figure 4 shows the RSSI training flowchart for designing BF methods. The DNN dataset for the scenario of the channel model can be described as; the training set consisting of 80% of the original size of the DNN dataset. The remaining ones are divided into testing which consists of 10% of the original size of the DNN dataset and validation which consists of 10% of the original size of the DNN dataset. Performance as a test set and valid set has been evaluated based on the use of both the test and validation data set.
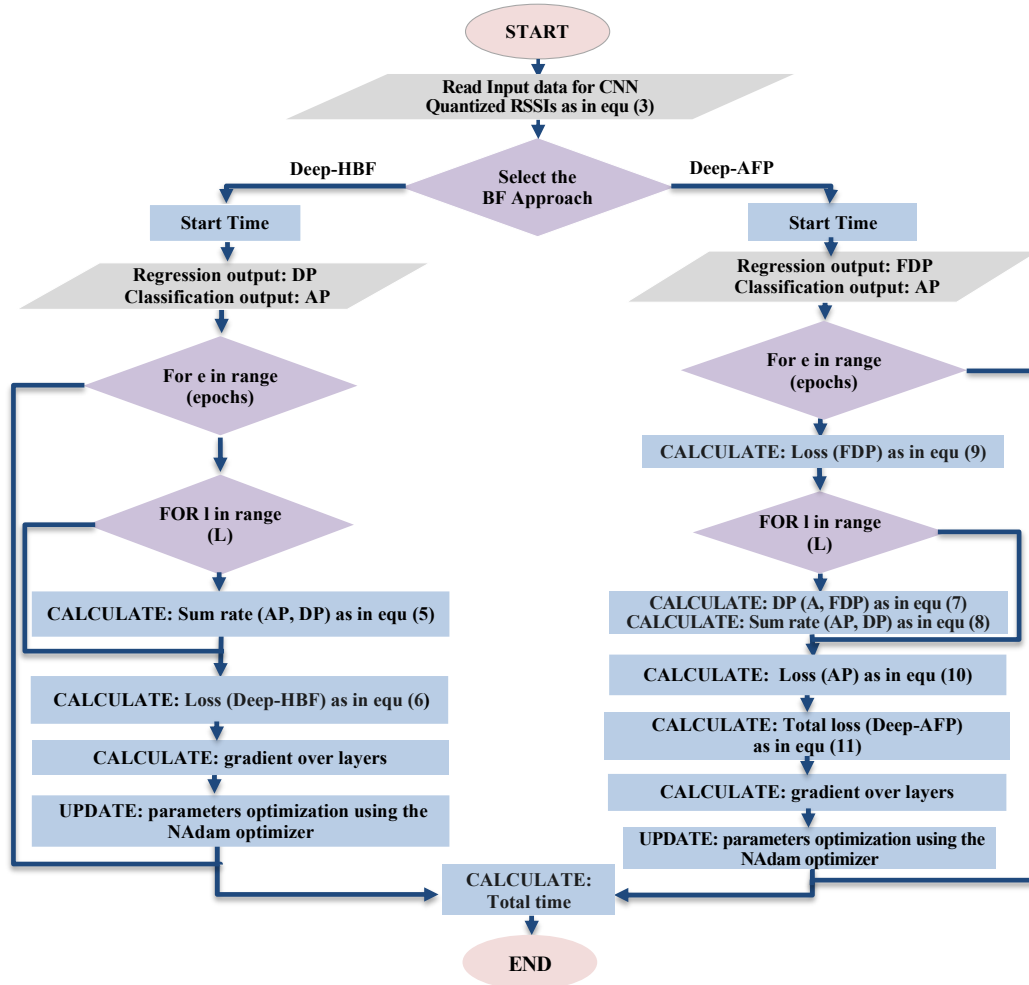
Figure 4. RSSI training flowchart for designing BF types

## 3.    RESULTS AND DISCUSSION

The performance of the two proposed BF architectures has been evaluated based on the sun rate calculation when the No. of users, $N_k$ is set as 4, the No. of antennas, $N_T$ is set as 64, the No. of RF chains, $N_{RF}$ is set as 8, the value of noise power, $N^2$ is set as -130 dBw and the average of SNRs is 14.35 dB. We require ($K \times N_k \times N_b$=1024 bits) for RSSI feedback where $N_b$ = 8 bits. A new RSSI method for designing HBF is implemented by PyTorch DL at Massive MIMO systems. The suggested work claims to have better performance in terms of SE than other techniques since minimal CSI feedback is required. The DNN has been implemented to compare the predicted value and optimum value of SE for two BF approaches. Six different models of optimizers have been planned with the specific goal of exploring the best model accuracy. The proposed CNN model has been utilized by using AdaDelta, Adam, AdaGrad, Nadam, RMSProp, and the stochastic gradient descent (SGD) optimizer. The accuracy of the proposed CNN model has been illustrated as shown in Figure 5, which measures how well the model predicts the correct output. It has been observed that the Nadam optimizer achieves the highest accuracy among all the optimizers, indicating that it produces more accurate predictions in the BF system. The accuracy of the proposed work has reached about 99.23%, with a higher value using the Nadam optimizer approach compared to other sex-different models of optimizers. This result indicates that the proposed research has improved the accuracy of the BF system over the latter by 0.81%. Furthermore, it has achieved a remarkable increase of 6.85% in performance over the RMSProp optimizer. Figure 6 presents the performance of each optimizer based on the loss metric, which quantifies the error between the predicted output and the actual output. A lower loss value suggests a better fit of the model to the data. The highest accuracy with the lowest loss has been achieved based on the most effective optimizer for the deep learning-based BF system. It is found that the Nadam optimizer achieves the lowest loss value of -5.208, indicating that it minimizes the error effectively and improves the overall performance of the BF system.
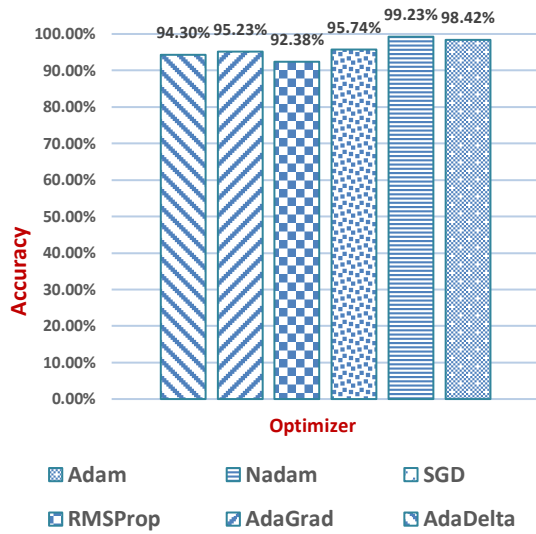
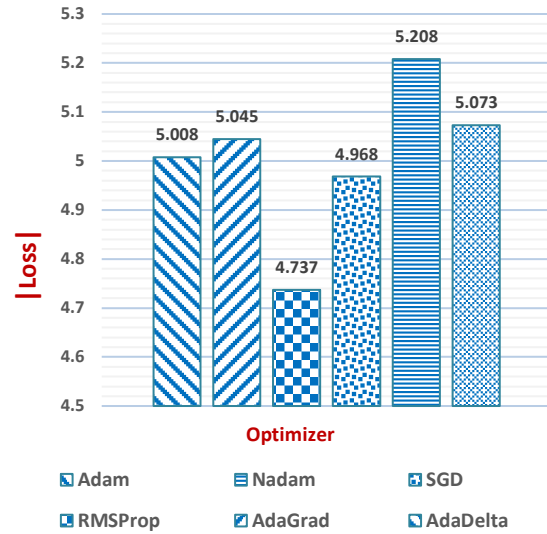Figure 5. Graphical chart for different accuracies of optimization



Figure 6. Graphical chart for different losses of optimization

Figures 7 and 8 illustrate the unsupervised loss that is used to train both AP tasks and DP or FDP tasks in both BF approaches. It is observed that the reduction in loss leads to an increase in average SE. The negative sign in the loss makes the DNN's training process focus on minimizing the loss function, which in turn maximizes the sum rate. Figure 7 illustrates the loss shape of the Deep-HBF network that was used to design the DP and AP directly from RSSIs with the number of iterations. The loss of Deep-HBF decreases over time, indicating that the algorithm is improving with each iteration. The progress of the Deep-HBF network in reducing the loss over time reached -5.208. Figure 8 presents the total loss of the Deep-AFP network, with the number of iterations reaching -10.271 concerning (11). The rate of decrease in loss may vary at different stages of the iteration. The loss function of this approach is used to design AP and DP based on the FDP. It is worth mentioning that the CSI can be used fully in training mode for loss calculation.
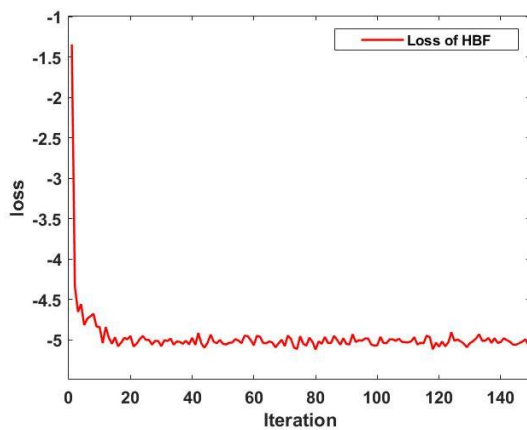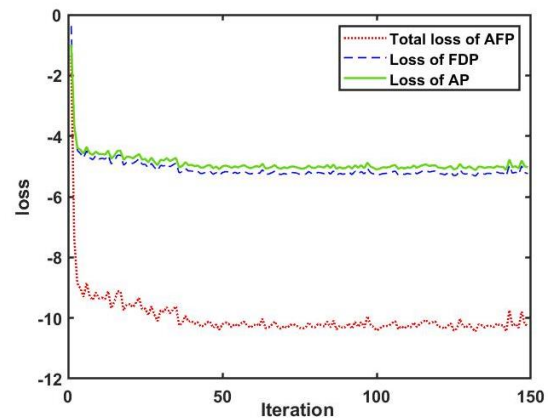


Figure 7. Loss with iteration No. for Deep-HBF



Figure 8. Loss with iteration No. for Deep-AFP

Figure 9 shows the achievable optimal values that can be achieved for the sum rate by Deep-HBF with different numbers of iterations. With this approach, the performance can be improved by reducing the loss with each iteration. Hence, it can be concluded that the performance of Deep-HBF achieves an accuracy of 99.23% with a predicted value of 5.23. Figure 10 illustrates the achievable optimum values for the sum rate by Deep-AFP with different numbers of iterations. It demonstrates the effectiveness of the Deep-AFP in reducing the loss and improving the accuracy of the BF process as the iterations progress. Hence, it can be

concluded that the performance of Deep-AFP achieves an accuracy of 95.42% with a predicted value of 5.38. Figure 11 visually demonstrates the comparison between the system performances of each approach, where Deep-HBF indicates a better performance outcome than other approaches. Figure 12 presents the sum-rate performance of BF designs versus a different logarithmic scale for power noise. It displays how changes in power noise impact the SE of the system. The Deep-AFP achieves high SE performance with different noise power values than other networks.
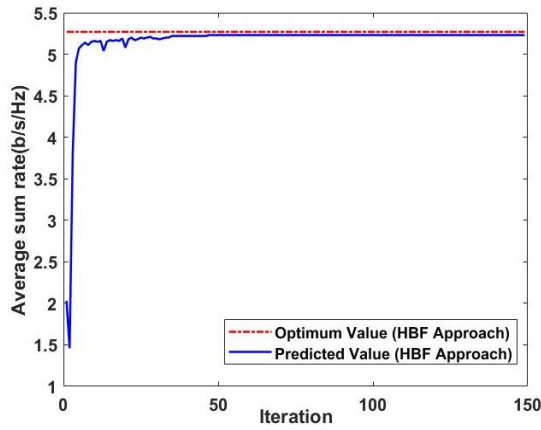


Figure 9. The optimum and predicted values for Deep-HBF
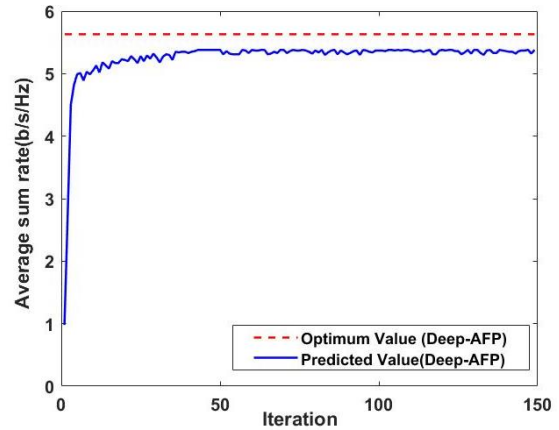


Figure 10. The optimum and predicted values for Deep-AFP
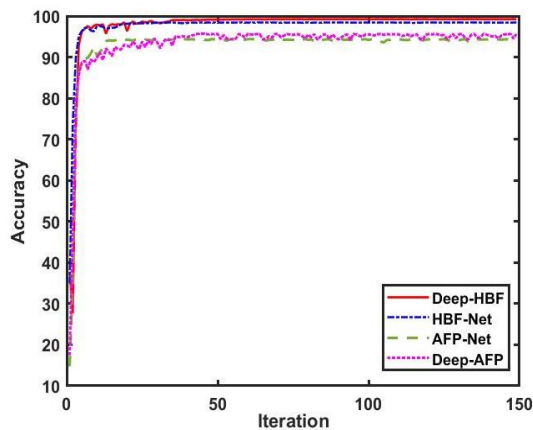


Figure 11. Performance accuracy of different methods for BF
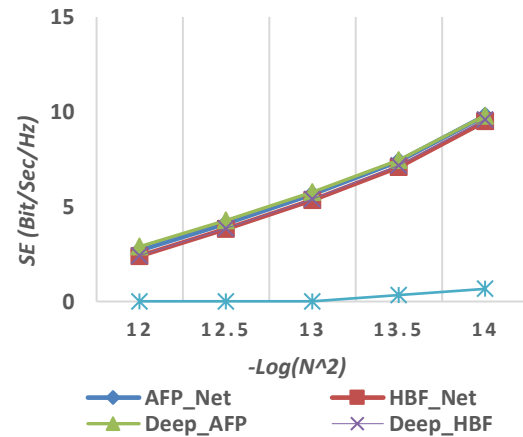


Figure 12. Sum-rate of BF types with different values of power noise

Based on the provided information, Table 2 compares the performance of different BF techniques, including the Deep-HBF, HBF-Net, Deep-AFP, and AFP-Net methods. The performance of DNN in each approach is exhibited for BF design by estimating the value of the accuracy of testing, validation, and runtime processing. The proposed Deep-HBF method achieves the highest test and valid spectral efficiencies with an accuracy of 99.23% and 99.03%, respectively, by reducing the learning rate to 1e-08. The runtime for the proposed Deep-HBF is 709.2914 sec. The accuracy of the proposed Deep-AFP achieves test and valid spectral efficiencies with an accuracy of 95.64% and 95.42%, respectively, with a runtime of 1425.864 sec. The results reveal that Deep-HBF performs better than HBF-Net by a rate of 0.81%, and Deep-HBF performs better than AFP-Net by a rate of 1.3%. However, he proposed that the approach of Deep-HBF has an increase in time of 87.1572 sec compared to HBF-Net. The approach of Deep-AFP has an increase in time (53.68 sec) compared to AFP-Net. Finally, the optimization process aimed at balancing the enhancement of the system's SE and the performance of DNNs. Remarkably, Deep-AFP outperformed AFP-Net by 0.06 in terms of SE, surpassed Deep-HBF by 0.15, and exceeded HBF-Net by 0.19. Moreover, Deep-HBF achieved an impressive

accuracy improvement of 0.81% compared to HBF-Net, a substantial gain of 3.81% over Deep-AFP, and a remarkable improvement of 4.89% when compared to AFP-Net. It is worth noting that the Deep-AFP network exhibited a higher range of computational complexity compared to the other networks. It has an increased runtime of (803.7298 sec) compared to the smallest runtime of the HBF-Net approach. Therefore, we need to look for an enhanced version of BF using DL that has little computational overhead and great performance.

Table 2. The comparison between the performances of the system for each approach

| Approach | Valid accuracy % | Test accuracy % | Runtime(s) |
|---|---|---|---|
| Proposed Deep-HBF | 99.03 | 99.23 | 709.2914 |
| HBF-Net [23] | 98.31 | 98.42 | 622.1342 |
| Proposed Deep-AFP | 95.42 | 95.64 | 1425.864 |
| AFP-Net [23] | 93.07 | 94.34 | 1372.184 |

## 4. CONCLUSION AND FUTURE WORK

In the paper, new insight into BF design was provided by using DL. A two-approach BF scheme is designed to obtain the optimal performance for BF, which is a key technology that increases the SE for Massive MIMO systems. The simulation results showed that the proposed performance of BF despite the lack of CSI, designed BF through BS training with near-optimal sum rates. Finally, therefore, a trade-off between enhancement SE of the system and the DNNs performance has been optimized and found that the Deep-HBF achieved an optimum accuracy with 99.23% for prediction value with a low computational complexity of 709.2914 sec represented in processing time than HBF-Net. The Deep-AFP achieved an optimum accuracy with 95.64% for prediction value with a low computational complexity of 1425.864 sec represented in processing time than AFP-Net. The Deep-Net has better SE compared to other approaches. In future work, efforts should be directed toward developing an improved version of BF via DL that achieves a high level of performance with minimal computational requirements. This can be achieved by improving and expanding DL-based BF capabilities, focusing on innovative architectures, algorithms, and training techniques. It is worth noting the possibility of using a new database with different specifications in an alternative environment to evaluate the performance of DNNs, paving the way for more efficient and adaptable wireless communication systems.

## REFERENCES

[1] S. Alraih, R. Nordin, A. Abu-Samah, I. Shayea, and N. F. Abdullah, "A survey on handover optimization in beyond 5G mobile networks: challenges and solutions," *IEEE Access*, vol. 11, pp. 59317–59345, 2023, doi: 10.1109/access.2023.3284905.

[2] A. F. Molisch *et al.*, "Hybrid beamforming for Massive MIMO: A survey," *IEEE Communications Magazine*, vol. 55, no. 9, pp. 134–141, 2017, doi: 10.1109/mcom.2017.1600400.

[3] C. Zhang, Y.-H. Huang, F. Sheikh, and Z. Wang, "Advanced baseband processing algorithms, circuits, and implementations for 5G communication," *IEEE Journal on Emerging and Selected Topics in Circuits and Systems*, vol. 7, no. 4, pp. 477–490, Dec. 2017, doi: 10.1109/jetcas.2017.2743107.

[4] A. H. Nalband, M. Sarvagy, and M. R. Ahmed, "Power saving and optimal hybrid precoding in millimeter wave Massive MIMO systems for 5G," *TELKOMNIKA (Telecommunication Computing Electronics and Control)*, vol. 18, no. 6, p. 2842, Dec. 2020, doi: 10.12928/telkomnika.v18i6.15952.

[5] C. Qi, Q. Liu, X. Yu, and G. Y. Li, "Hybrid precoding for mixture use of phase shifters and switches in mmWave Massive MIMO," *IEEE Transactions on Communications*, vol. 70, no. 6, pp. 4121–4133, Jun. 2022, doi: 10.1109/tcomm.2022.3173304.

[6] Z. Lin, X. Du, H.-H. Chen, B. Ai, Z. Chen, and D. Wu, "Millimeter-wave propagation modeling and measurements for 5G mobile networks," *IEEE Wireless Communications*, vol. 26, no. 1, pp. 72–77, Feb. 2019, doi: 10.1109/mwc.2019.1800035.

[7] S. Han, C. I, Z. Xu, and C. Rowell, "Large-scale antenna systems with hybrid analog and digital beamforming for millimeter wave 5G," *IEEE Communications Magazine*, vol. 53, no. 1, pp. 186–194, Jan. 2015, doi: 10.1109/mcom.2015.7010533.

[8] İ. Yazici, I. Shayea, and J. Din, "A survey of applications of artificial intelligence and machine learning in future mobile networks-enabled systems," *Engineering Science and Technology, an International Journal*, vol. 44, p. 101455, Aug. 2023, doi: 10.1016/j.jestch.2023.101455.

[9] M. Naeem, G. De Pietro, and A. Coronato, "Application of reinforcement learning and deep learning in multiple-input and multiple-output (MIMO) systems," *Sensors*, vol. 22, no. 1, p. 309, Dec. 2021, doi: 10.3390/s22010309.

[10] J. Zhang, G. Zheng, Y. Zhang, I. Krikidis, and K.-K. Wong, "Deep learning based predictive beamforming design," *IEEE Transactions on Vehicular Technology*, vol. 72, no. 6, pp. 8122–8127, Jun. 2023, doi: 10.1109/tvt.2023.3238108.

[11] C.-K. Wen, W.-T. Shih, and S. Jin, "Deep learning for Massive MIMO CSI feedback," *IEEE Wireless Communications Letters*, vol. 7, no. 5, pp. 748–751, Oct. 2018, doi: 10.1109/lwc.2018.2818160.

[12] I. Ahmed, M. K. Shahid, H. Khammari, and M. Masud, "Machine learning based beam selection with low complexity hybrid beamforming design for 5G Massive MIMO systems," *IEEE Transactions on Green Communications and Networking*, vol. 5, no. 4, pp. 2160–2173, Dec. 2021, doi: 10.1109/tgcn.2021.3093439.

[13] M. S. Aljumaily and H. Li, "Machine learning aided hybrid beamforming in massive-MIMO millimeter wave systems," in *2019 IEEE International Symposium on Dynamic Spectrum Access Networks (DySPAN)*, IEEE, Nov. 2019. doi: 10.1109/dyspan.2019.8935814.

[14] F. Liang, C. Shen, W. Yu, and F. Wu, "Towards optimal power control via ensembling deep neural networks," *IEEE Transactions on Communications*, vol. 68, no. 3, pp. 1760–1776, Mar. 2020, doi: 10.1109/tcomm.2019.2957482.

[15] A. Alkhateeb, S. Alex, P. Varkey, Y. Li, Q. Qu, and D. Tujkovic, "Deep learning coordinated beamforming for highly-mobile millimeter wave systems," *IEEE Access*, vol. 6, pp. 37328–37348, 2018, doi: 10.1109/access.2018.2850226.

[16] Y. Zhang, A. Liu, P. Li, and S. Jiang, "Deep learning (DL)-based channel prediction and hybrid beamforming for LEO satellite Massive MIMO system," *IEEE Internet of Things Journal*, vol. 9, no. 23, pp. 23705–23715, Dec. 2022, doi: 10.1109/jiot.2022.3190412.

[17] C. Huang, G. C. Alexandropoulos, C. Yuen, and M. Debbah, "Indoor signal focusing with deep learning designed reconfigurable intelligent surfaces," in *2019 IEEE 20th International Workshop on Signal Processing Advances in Wireless Communications (SPAWC)*, IEEE, Jul. 2019. doi: 10.1109/spawc.2019.8815412.

[18] T. Lin and Y. Zhu, "Beamforming design for large-scale antenna arrays using deep learning," *IEEE Wireless Communications Letters*, vol. 9, no. 1, pp. 103–107, Jan. 2020, doi: 10.1109/lwc.2019.2943466.

[19] Remcom, "Wireless InSite® 3D Wireless Propagation Software," *Remcom*. https://www.remcom.com/wireless-insite-propagation-software (accessed Nov. 23, 2023).

[20] A. Alkhateeb, "DeepMIMO: A generic deep learning dataset for millimeter wave and Massive MIMO applications," *arXiv*, pp. 1–8, Feb. 2019, Accessed: Jun. 20, 2024. [Online]. Available: https://arxiv.org/abs/1902.06435v1

[21] J.-C. Chen, "Hybrid beamforming with discrete phase shifters for millimeter-wave Massive MIMO systems," *IEEE Transactions on Vehicular Technology*, vol. 66, no. 8, pp. 7604–7608, Aug. 2017, doi: 10.1109/tvt.2017.2670638.

[22] H. Hojatian, V. N. Ha, J. Nadal, J.-F. Frigon, and F. Leduc-Primeau, "RSSI-based hybrid beamforming design with deep learning," in *ICC 2020 - 2020 IEEE International Conference on Communications (ICC)*, IEEE, Jun. 2020. doi: 10.1109/icc40277.2020.9149321.

[23] H. Hojatian, J. Nadal, J.-F. Frigon, and F. Leduc-Primeau, "Unsupervised deep learning for Massive MIMO hybrid beamforming," *IEEE Transactions on Wireless Communications*, vol. 20, no. 11, pp. 7086–7099, Nov. 2021, doi: 10.1109/twc.2021.3080672.

[24] D. Zhang, Y. Wang, X. Li, and W. Xiang, "Hybrid beamforming for downlink multiuser millimetre wave MIMO-OFDM systems," *IET Communications*, vol. 13, no. 11, pp. 1557–1564, Jul. 2019, doi: 10.1049/iet-com.2018.6061.

[25] Z. Amirifar and J. Abouei, "An improvement to hybrid beamforming precoding scheme for mmWave Massive MIMO systems based on channel matrix," *Indonesian Journal of Electrical Engineering and Computer Science*, vol. 23, no. 1, p. 285, Jul. 2021, doi: 10.11591/ijeecs.v23.i1.pp285-292.

[26] A. Singh and S. Joshi, "A survey on hybrid beamforming in MmWave Massive MIMO system," *Journal of scientific research*, vol. 65, no. 01, pp. 201–213, 2021, doi: 10.37398/jsr.2021.650126.

[27] H. Hojatian, Z. Mlika, J. Nadal, J.-F. Frigon, and F. Leduc-Primeau, "Learning energy-efficient hardware configurations for Massive MIMO beamforming," *arXiv*, Aug. 2023, Accessed: Jun. 20, 2024. [Online]. Available: http://arxiv.org/abs/2308.06376

[28] M. Shehata, A. Mokh, M. Crussiere, M. Helard, and P. Pajusco, "On the equivalence between hybrid and full digital beamforming in mmWave communications," in *2019 26th International Conference on Telecommunications (ICT)*, IEEE, Apr. 2019. doi: 10.1109/ict.2019.8798794.

[29] M. Gustineli, "A survey on recently proposed activation functions for deep learning," *arXiv*, Apr. 2022, Accessed: Jun. 20, 2024. [Online]. Available: http://arxiv.org/abs/2204.02921

[30] S. R. Dubey, S. K. Singh, and B. B. Chaudhuri, "Activation functions in deep learning: A comprehensive survey and benchmark," *Neurocomputing*, vol. 503, pp. 92–108, Sep. 2022, doi: 10.1016/j.neucom.2022.06.111.

[31] A. D. Jagtap and G. E. Karniadakis, "How important are activation functions in regression and classification? a survey, performance comparison, and future directions," *Journal of Machine Learning for Modeling and Computing*, vol. 4, no. 1, pp. 21–75, 2023, doi: 10.1615/jmachlearnmodelcomput.2023047367.

## BIOGRAPHIES OF AUTHORS

**Ibrahim El-Metwally Ramadan** 🆔 📇 SC 🔗 is a teaching assistant at the Communications and Electronics Engineering Department, Misr Higher Institute for Engineering and Technology, Faculty of Engineering, Mansoura, Egypt. He received an M.Sc. degree in communications engineering from Mansoura University in 2018. His research of interest is concerned with the following topics: Mobile communication, wireless sensor networks, signal processing, and optical communication. He can be contacted at: i.elmatwally89@gmail.com.

**Eman AbdElhalim** 🆔 📇 SC 🔗 is an assistant professor, in the Electronics and Communications Department, Faculty of Engineering. Her research interests cover several aspects of communications, cloud computing, big data analytics, and medical imaging using deep learning techniques. Dr. Eman is a reviewer of more than 10 peer-reviewed publications appearing in reputable journals. Eman teaches several courses on artificial intelligence, signal processing, and programming. Eman also organized workshops on applications of artificial intelligence in industry and production environments. She is training several sessions in digital transformation. She has been working since 2008 on graduation projects in the field of applications of deep learning in communications and medical imaging fields. She can be contacted at email: eman_haleim@mans.edu.eg.

**Ahmed Ibrahim Saleh** 🆔 ⁸ˢᶜ ℃ received a B. Sc. in computer engineering and control systems from Mansoura University, Egypt with a general grade of excellent. He got a master's degree and a PhD degree in the area of mobile agent and computing. His research interests include (programming languages, networks and system administration, and database), he is currently a professor in the Faculty of Engineering, at Mansoura University. Po. Box: 35516. He can be contacted at email: aisaleh@yahoo.com.

**Hossam El-Din Salah Moustafa** 🆔 ⁸ˢᶜ ℃ is a professor at the Department of Electronics and Communications Engineering, the founder and former executive manager of the Biomedical Engineering Program (BME) at the Faculty of Engineering, Mansoura University. He is an IEEE senior member. Research interests include biomedical imaging, image processing applications, and bioinformatics. He can be contacted at email: hossam-moustafa@hotmail.com.